CrossMark

Effects of Vertical Throughflow and Variable Gravity on Hadley–Prats Flow in a Porous Medium

N. Deepika[1] · P. A. L. Narayana[1]

Abstract The stability of convection in a horizontal porous layer which is saturated with fluid and induced by horizontal temperature gradients subjected to horizontal mass flow is investigated by means of linear and nonlinear stability analysis. The effects of variable gravity field and vertical throughflow are also considered in this analysis. The nonlinear stability analysis part has been developed via energy functional. Shooting and Runge–Kutta methods have been used to solve eigenvalue problem in both cases. Critical vertical thermal Rayleigh numbers for both linear and nonlinear analyses R_{L} and R_{E} are evaluated for different values of horizontal Rayleigh number R_x, horizontal Peclet number Pe, vertical Peclet number Q_{v} and variable gravity parameter η. Comparison is made between linear and nonlinear stability results. It has been observed that linear stability results are overpredicting the onset of convection compared with nonlinear theory, and hence subcritical instabilities would arise before one gets the onset of linear stability threshold.

Keywords Hadley–Prats flow · Linear stability · Nonlinear stability · Energy method · Porous medium

List of symbols

c	Specific heat
$\mathbf{g}$	Gravitational acceleration
H	Height of porous layer
k	Wave number in x direction
l	Wave number in y direction
k_m	Thermal conductivity

✉ P. A. L. Narayana
ananth@iith.ac.in

N. Deepika
deepika.neela@gmail.com

[1] Indian Institute of Technology Hyderabad, Yeddumailaram 502 205, Telangana, India

🖄 Springer

K	Permeability of the medium
P	Pressure
Pe	Horizontal Peclet number
Q_v	Vertical Peclet number
T	Temperature
t	Time
$\mathbf{v} = (u, v, w)$	Velocity vector
V	Periodicity cell
R_x	Horizontal thermal Rayleigh number
R_z	Vertical thermal Rayleigh number
(x, y, z)	Cartesian coordinates

Greek symbols

α	Overall wave number
α_m	Thermal diffusivity
β	Horizontal thermal gradient
η	Variable gravity coefficient
γ_T	Thermal expansion coefficient
μ	Viscosity
ρ	Density
θ	Perturbation in temperature
ξ	Coupling parameter

Subscripts

| m | Porous medium |
| f | Fluid medium |

Superscripts

| $*$ | Dimensional quantity |
| $'$ | Perturbation |

1 Introduction

The study of buoyancy-driven flows in the porous media is vital since it has numerous applications in fields like insulation of buildings, geothermal reservoirs, and chemical reactor engineering. Natural convection in a porous layer by heating from below was first studied by Horton and Rogers (1945) and Lapwood (1948) which is known as Horton–Rogers–Lapwood (H–R–L) problem. In this study, they have investigated on a homogeneous and isotropic porous layer with uniform thickness in which Darcy law, Oberbeck-Boussinesq approximation, and local thermal equilibrium condition are valid. There are many extensions to this problem with inclusion of additional effects such as inclined temperature gradients, inclined porous layer, viscous dissipation, mass flow, local thermal non- equilibrium.

Later, Prats (1966) studied the effect of horizontal fluid flow on convection in a porous layer. Then after, Weber (1974) investigated the stability of convection induced by inclined temperature gradients assuming them as small in magnitude. This problem is more complicated than the model considered in the H–R–L problem or pure Darcy–Benard convection. In

problems of this type, temperature field is assumed to vary linearly in the horizontal direction. And that non-uniformity in the horizontal temperature induces a flow into basic solution. The flow generated by these gradients is referred to as Hadley flow. Nield (1991, 1994) got rid of the limitation on horizontal temperature gradients which were to be small, and the resultant eigenvalue problem in both cases was solved by using two-term Galerkin approximation. When Hadley flow is subjected to horizontal mass flow, it leads to Hadley–Prats flow. A book by Nield and Bejan (2013) mentioned all the improvements in this area of research.

Investigation of effect of vertical throughflow is important since it gives a possibility to control the convective instability with adjustment of throughflow. This type of study has applications in packed bed reactors. Effect of throughflow in a porous medium was first studied by Wooding (1960) where the domain was semi-infinite in the vertical direction, and this study was followed by Sutton (1970) and Chen (1990). It was further extended by Nield (1998) with inclined temperature gradients by concluding that the effect of throughflow is independent of its direction when both the upper and lower boundary conditions are identical. Nield and Kuznetsov (2013) investigated throughflow on convection in a porous medium which consisted two horizontal porous layers. All the above studies are based on the Darcy flow model in which inertia and viscous dissipation effects are neglected. Barletta et al. (2010) investigated on thermal convection with effect of viscous dissipation in the energy balance and also with vertical throughflow. Khalili and Shivakumara (2003) employed Brinkman-extended Darcy model to study the effect of vertical throughflow. Rees and Bassom (2000) studied Darcy–Bénard problem where the porous layer was inclined to some angle. Brevdo and Ruderman (2009) analyzed the destabilization of transverse modes when the flow undergoes the effect of vertical throughflow. Most of the above works were concentrated only on the effect of either horizontal mass flow or vertical throughflow. But the present article aims at studying both the effects simultaneously.

When the gravity field varies with the height of the porous layer, the buoyancy force exerted by the fluid also varies. This leads to a situation where some part of the fluid layer will tendency to become stable and the remaining part unstable. Hence, in large-scale convection problems, it is essential to take account of variation of gravity with height. Alex et al. (2001) analyzed variable gravity effects on convection in isotropic porous layer with internal heat source. Later on, it was extended to anisotropic porous layer in the article by Alex and Patil (2002). Variable gravity effects was studied by Straughan (1989), Kaloni and Qiao (2001) and Harfash (2014).

Most of the above contributions are restricted to linear theory. It is a known fact that the energy method and the linear stability theory complement each other in demarking the range of parameter space in which the subcritical instabilities would arise. Nonlinear stability theory using energy functional overcomes the drawbacks in the linear stability analysis. Nonlinear analysis by energy method may be found in Straughan (2004). Homsy and Sherwood (1976) analyzed the convective instability in a porous medium confined between isothermal boundaries, using linear instability theory and nonlinear stability theory. Straughan (1989) added the effect of variable gravity field to the convection problem and examined linear and nonlinear stability analyses and observed that there is a small bandwidth where possible subcritical instabilities arise. Several researchers have studied the nonlinear stability by using the energy method. Kaloni and Qiao (1997), Qiao and Kaloni (1998), and Kaloni and Qiao (2000) extended this in various phases by including effect of inclined temperature gradients, vertical throughflow, and thermosolutal convection with horizontal mass flow, respectively. Harfash (2014) studied the convection in a fluid-saturated porous media by using linear and nonlinear analyses with the effects of internal heat source, variable gravity.

The aim of present article is to study the onset of convection with horizontal mass flow, vertical throughflow, and variable gravity effect by using linear and nonlinear stability analyses. In this discussion, Sect. 2 deals with governing equations and steady-state solution, Sects. 3 and 4 with the linear and nonlinear stability analyses, and Sect. 5 with numerical solution of the eigenvalue problems and discussion of results.

2 Mathematical Formulation

A horizontal fluid-saturated homogeneous porous layer with thickness H is considered. Cartesian system has its z^*-axis vertically upwards which opposes the direction of gravity and x^*-axis is in the direction of imposed horizontal temperature gradient β. The porous layer extends to infinity in horizontal directions, and bounded by permeable plates $z^* = H/2$ and $z^* = -H/2$. The vertical temperature difference between the plates be ΔT. The schematic diagram of the problem is shown in Fig. 1. The flow in the porous medium is governed by Darcy law. Oberbeck–Boussinesq approximation is valid that means the density variations are sufficiently small to be neglected everywhere except in the body force term, and density is given by

$$\rho_f{}^* = \rho_0 \left[1 - \gamma_T \left(T^* - T_0\right)\right], \tag{1}$$

where T^* is the temperature, $\rho_f{}^*$ is the fluid density, ρ_0 is the density at temperature T_0, and γ_T is the volumetric thermal expansion coefficient. It is assumed that the gravity vector varies linearly with z^* i.e.,

$$\begin{aligned} \mathbf{g} &= g_0 h(z^*)\mathbf{k} \\ &= -g_0 \left(1 + \eta \frac{z^*}{H}\right)\mathbf{k}, \end{aligned} \tag{2}$$

where g_0 is the constant gravitational acceleration, η is the variable gravity coefficient, and $\mathbf{k}$ is the unit vector in vertical direction. The governing equations in dimensional form are

$$\nabla^* \cdot \mathbf{v}^* = 0, \tag{3}$$

$$\frac{\mu}{K}\mathbf{v}^* = -\nabla^* P^* + \rho_f{}^*\mathbf{g}, \tag{4}$$

$$(\rho c)_m \frac{\partial T^*}{\partial t^*} + (\rho c_p)_f (\mathbf{v}^* \cdot \nabla^* T^*) = k_m \nabla^{*2} T^*, \tag{5}$$
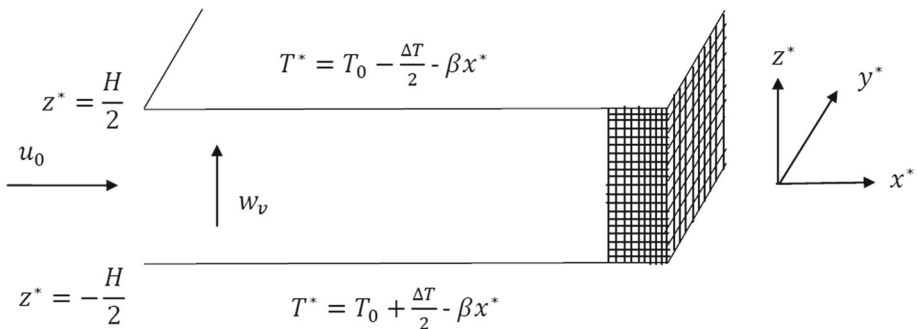

Fig. 1 Sketch of the porous medium

where $\mathbf{v}^* = (u^*, v^*, w^*)$, P^* are the seepage velocity and pressure, respectively. The subscripts m and f indicates to the porous medium and fluid, respectively. In addition, μ, c, k_m, and K stand for viscosity, specific heat, thermal conductivity and permeability of the medium, respectively. It is supposed that there is a throughflow with velocity w_v in the vertical direction, and then the boundary conditions are in the form

$$z^* = \pm \frac{H}{2} : \quad w^* = w_v, \quad T^* = T_0 - \frac{(\pm \Delta T)}{2} - \beta x^*. \tag{6}$$

Now, the following non-dimensional variables are introduced to non-dimensionalize the governing equations (3)–(6)

$$(x, y, z) = \frac{1}{H}(x^*, y^*, z^*), \quad t = \frac{\alpha_m}{AH^2}t^*, \quad (u, v, w) = \mathbf{v} = \frac{H}{\alpha_m}\mathbf{v}^*,$$

$$P = \frac{K(P^* + \rho_0 \mathbf{g} z^*)}{\mu \alpha_m}, \quad T = \frac{R_z(T^* - T_0)}{\Delta T},$$

$$\alpha_m = \frac{k_m}{(\rho c_p)_f}, \quad A = \frac{(\rho c)_m}{(\rho c_p)_f}, \tag{7}$$

The above scaling leads to the following non-dimensional parameters

$$Q_v = \frac{w_v H}{\alpha_m}, \quad Pe = \frac{u_0 H}{\alpha_m},$$

$$R_z = \frac{\rho_0 g_0 \gamma_T K H \Delta T}{\mu \alpha_m}, \quad R_x = \frac{\rho_0 g_0 \gamma_T K H^2 \beta}{\mu \alpha_m}. \tag{8}$$

Here Q_v, Pe are vertical and horizontal Peclet numbers and R_z, R_x are vertical and horizontal Rayleigh numbers. The flow governing equations representing conservation of mass, momentum, and energy balance are in the form

$$\nabla \cdot \mathbf{v} = 0, \tag{9}$$

$$\mathbf{v} = -\nabla P + T(1 + \eta z)\mathbf{k}, \tag{10}$$

$$\frac{\partial T}{\partial t} + \mathbf{v} \cdot \nabla T = \nabla^2 T. \tag{11}$$

The corresponding boundary conditions are

$$z = \pm \frac{1}{2} : \quad w = Q_v, \quad T = -\frac{(\pm R_z)}{2} - R_x x. \tag{12}$$

The basic steady-state solution $(\mathbf{v}_s, P_s, T_s)$ of Eqs. (9)–(12) are in the form

$$u_s = R_x \left(z + \eta \frac{z^2}{2} - \frac{\eta}{24} \right) + Pe, \quad v_s = 0, \quad w_s = Q_v, \quad P_s = P(x, y, z), \tag{13}$$

$$T_s = -R_x x + Az^3 + Bz^2 + Cz + D - (R_z + E)\frac{(\exp(Q_v z) - \cosh(Q_v/2))}{F}. \tag{14}$$

A constraint is imposed to be there is a net mass flow in the x direction, in such a way that

$$\int_{-1/2}^{1/2} u_s = Pe, \quad \int_{-1/2}^{1/2} v_s = 0. \tag{15}$$

The basic state solution is given by Eqs. (13)–(14) which is commonly referred to as Hadley–Prats flow. Vertical temperature gradient is given by

$$DT_s = \frac{dT_s}{dz} = \begin{cases} -4G\eta z^3 - 12Gz^2 + (G\eta - R_x Pe)z + (-R_z + G), & \text{for } Q_v = 0, \\ 3Az^2 + 2Bz + C - ((R_z + E)/F)Q_v \exp(Q_v z), & \text{for } Q_v \neq 0. \end{cases}$$

where

$$A = \frac{R_x{}^2 \eta}{6Q_v}, \quad B = \frac{R_x{}^2}{2}\left(\frac{\eta}{Q_v{}^2} + \frac{1}{Q_v}\right),$$

$$C = \left[R_x{}^2\left(\frac{\eta}{Q_v{}^3} + \frac{1}{Q_v{}^2} - \frac{\eta}{24Q_v}\right) + \frac{R_x Pe}{Q_v}\right], \quad D = -\frac{R_x{}^2}{8}\left(\frac{\eta}{Q_v{}^2} + \frac{1}{Q_v}\right),$$

$$E = \frac{R_x{}^2 \eta}{24Q_v} + R_x{}^2\left(\frac{\eta}{Q_v{}^3} + \frac{1}{Q_v{}^2} - \frac{\eta}{24Q_v}\right) + \frac{R_x Pe}{Q_v},$$

$$F = 2\sinh(Qv/2), \quad G = \frac{R_x{}^2}{24}.$$

Now, the following perturbations to the basic solution are imposed as

$$\mathbf{v} = \mathbf{v}_s + \mathbf{v}', \quad T = T_s + \theta, \quad P = P_s + p'. \tag{16}$$

where the prime denotes a very small perturbation parameter. The perturbation equations are

$$\nabla \cdot \mathbf{v}' = 0, \tag{17}$$

$$\mathbf{v}' = -\nabla p' + (1 + \eta z)\theta\mathbf{k}, \tag{18}$$

$$\frac{\partial \theta}{\partial t} + \mathbf{v}_s \cdot \nabla\theta + \mathbf{v}' \cdot \nabla T_s + \mathbf{v}' \cdot \nabla\theta = \nabla^2\theta, \tag{19}$$

and the corresponding boundary conditions are

$$z = \pm\frac{1}{2}: \quad w' = \theta = 0. \tag{20}$$

Eq. (20) represents zero perturbations on the velocity, temperature at the lower and upper plates.

3 Linear Stability Analysis

In order to perform the linear stability analysis, the products of perturbations are neglected in the system (17)–(19). The resultant linearized perturbation equations are subjected to small wave-like perturbations in the form

$$(u', v', w', \theta, p') = (u(z), v(z), w(z), \theta(z), p(z)) \exp i(kx + ly - \sigma t). \tag{21}$$

where $i = \sqrt{-1}$, k, and l are wave numbers in x and y directions, respectively, and σ is a complex growth rate parameter. On substituting Eq. (21) and eliminating $u(z)$, $v(z)$, and $p(z)$, the corresponding eigenvalue problem is derived as follows

$$(D^2 - \alpha^2)w + \alpha^2(1 + \eta z)\theta = 0, \tag{22}$$

$$(D^2 - \alpha^2 + i\sigma - iku_s)\theta + i\frac{kR_x}{\alpha^2}Dw - DT_sw - Q_vD\theta = 0, \tag{23}$$

$$z = \pm\frac{1}{2}: \quad w = \theta = 0. \tag{24}$$

where $D = d/dz$ and $\alpha = \sqrt{k^2 + l^2}$ is the overall wave number. In this study, $k = 0$ referred to as a longitudinal mode and $l = 0$ as a transverse mode. The system of Eqs. (22)–(24) constitutes an eigenvalue problem for vertical thermal Rayleigh number R_z and in this problem R_z appears through the term DT_s.

4 Nonlinear Stability Analysis

While carrying out the nonlinear energy stability analysis with considering all perturbations, an energy functional is defined as

$$E(t) = \frac{\xi}{2}\|\theta\|^2, \tag{25}$$

where ξ is a coupling parameter. On multiplying Eq. (18) by $\mathbf{v}'$, Eq. (19) by θ and integrating over V by using boundary conditions and Gauss divergence theorem, the following equations are yielded

$$\|\mathbf{v}'\|^2 = \langle(1 + \eta z)\theta w'\rangle, \tag{26}$$

$$\frac{1}{2}\frac{d}{dt}\|\theta\|^2 = -\|\nabla\theta\|^2 - \langle(\mathbf{v}' \cdot \nabla T_s)\theta\rangle. \tag{27}$$

where V indicates periodicity cell, $\langle.\rangle$ denotes integration over V, and $\|.\|$ denotes the $L^2(V)$ norm. The Eqs. (26)–(27) along with Eq. (25) can be written as

$$\frac{dE}{dt} = I - D, \tag{28}$$

where

$$I = \langle(1 + \eta z)\theta w'\rangle - \xi\langle(\mathbf{v}' \cdot \nabla T_s)\theta\rangle, \tag{29}$$

$$D = \xi\|\nabla\theta\|^2 + \|\mathbf{v}'\|^2. \tag{30}$$

Therefore,

$$\frac{dE}{dt} = D\left(\frac{I}{D} - 1\right)$$

$$\leq -D\left(1 - \max_H \frac{I}{D}\right). \tag{31}$$

where H is a set of all admissible solutions over which it is looked for maximum, further $H = (\mathbf{v}', \theta) \in L^2(V): \nabla.\mathbf{v}' = 0, \mathbf{v}' = \theta = 0$ at $z = \pm\frac{1}{2}$. Eq. (28) becomes the following maximization problem

$$m = \max_H \frac{I}{D}, \tag{32}$$

Eq. (31) becomes

$$\frac{dE}{dt} \leq -D(1-m),$$

By using Poincare inequality $\pi^2 \|\theta\|^2 \leq \|\nabla\theta\|^2$, from Eq. (31), the following inequality is arrived.

$$\frac{dE}{dt} \leq -2\pi^2(1-m)E, \tag{33}$$

By integrating above equation, and $0 < m < 1$,

$$E(t) \leq e^{-2\pi^2(1-m)t}E(0). \tag{34}$$

Inequality (34) shows $E(t) \to 0$ exponentially as $t \to \infty$ for $0 < m < 1$. In Eq. (32), assuming the critical argument $m = 1$. Then the maximization problem becomes

$$\delta I - m\delta D = 0. \tag{35}$$

The associated Euler–Lagrange equations are

$$(1 + \eta z)\theta\mathbf{k} - \xi\nabla T_s\theta - 2\mathbf{v}' = \nabla\lambda, \tag{36}$$

$$(1 + \eta z)w' - \xi(\mathbf{v}' \cdot \nabla T_s) + 2\xi\nabla^2\theta = 0, \tag{37}$$

where λ is a Lagrange multiplier which is introduced because $\mathbf{v}'$ is solenoidal. By applying *curlcurl* to Eq. (36) and taking third component of resulting equation, the following equation is obtained.

$$\xi DT_s\nabla_1^2\theta - (1 + \eta z)\nabla_1^2\theta + 2\nabla_1^2 w' - 2\frac{\partial}{\partial z}\left(\frac{\partial u'}{\partial x} + \frac{\partial v'}{\partial y}\right) + \xi R_x\frac{\partial^2\theta}{\partial x\partial z} = 0, \tag{38}$$

where

$$\nabla_1^2 = \frac{\partial^2}{\partial x^2} + \frac{\partial^2}{\partial y^2}.$$

Now employing the normal modes (21) to Eqs. (37) and (38) and eliminating the variables u, v and λ, we arrived at the following equations.

$$\left(D^2 - \alpha^2\right)w + \frac{1}{2}(1 + \eta z)\alpha^2\theta + \frac{ik\xi}{2}R_x D\theta - \frac{\xi\alpha^2}{2}DT_s\theta = 0, \tag{39}$$

$$\left(D^2 - \alpha^2\right)\theta + \frac{1}{2\xi}(1 + \eta z)w + \frac{\xi}{4}R_x^2\theta - \frac{1}{2}DT_sw = 0, \tag{40}$$

$$z = \pm\frac{1}{2}: \quad w = \theta = 0. \tag{41}$$

Eqautions (39)–(41) forms an eigenvalue problem for R_z.

5 Results and Discussion

We look for numerical solution of eigenvalue problems (22)–(24) and (39)–(41) for linear and nonlinear cases, respectively, and R_z treated as eigenvalue. Eigenvalue R_z is found for given a set of input parameters α, Pe, Q_v, R_x, η. In order to solve the eigenvalue problems,

Table 1 Comparison between Nield (1998), present linear theories; Kaloni and Qiao (1997) and present nonlinear theories

	$R_x = 0$	$R_x = 10$	$R_x = 20$	$R_x = 30$	$R_x = 40$
$Q_v = 0$					
Nield	39.48	42.01	49.56	62.01	79.02
Present	39.4784	42.0076	49.5486	61.9567	78.9662
Kaloni	39.4784	40.7235	44.2151	49.3234	55.2825
Present	39.4783	40.7234	44.2092	49.1855	53.6194
$Q_v = 1$					
Nield	40.88	43.40	50.94	63.34	80.31
Present	40.87501	43.40333	50.9402	63.3359	80.3161
$Q_v = 2$					
Nield	45.08	47.60	55.13	67.49	84.38
Present	45.0775	47.6031	55.1272	67.4862	84.3799
$Q_v = 3$					
Nield	52.07	54.58	62.08	74.38	91.12
Present	52.0684	54.5881	62.0877	74.3813	91.1274
$Q_v = 4$					
Nield	61.67	64.16	71.61	83.78	100.3
Present	61.66631	64.1709	71.6160	83.7856	100.278

shooting and Runge–Kutta methods are employed as given in Barletta et al. (2010). Critical Rayleigh number for both linear and nonlinear theories is as follows

$$R_L = \min_k \min_l R_z(k, l, R_x, \eta, Q_v, Pe),$$
$$R_E = \max_\xi \min_k \min_l R_z(k, l, R_x, \eta, Q_v, Pe, \xi).$$

Here ξ is chosen optimally as given in Kaloni and Qiao (2000). In this discussion, the response of critical vertical thermal Rayleigh numbers R_L and R_E is examined for various parameters in the case of stationary longitudinal modes ($\sigma = 0, k = 0$) because these are the only preferred modes observed by Nield (1991). In the absence of variable gravity ($\eta = 0$), the linear theory in the present problem reduces to the problem solved by Nield (1998). Table 1 a shows good agreement between Nield (1998) and the present linear theories. And also, in the absence of variable gravity, vertical throughflow ($\eta = 0, Q_v = 0$), present nonlinear theory, leads to the problem in Kaloni and Qiao (1997), and this comparison is shown in Table 1. Throughout discussion, dashed lines represent the linear stability theory and solid lines represent nonlinear stability theory.

Figure 2 shows the plot of critical vertical thermal Rayleigh numbers R_L and R_E versus vertical Peclet number Q_v for $Pe = 0$ and $R_x = 0$. The effect of variable- gravity parameter is displayed by comparison between $\eta = 0, 1$. When $Q_v > 0$ (upwardflow), the porous layer experiences hot fluid input, and hence global temperature increases. When $Q_v < 0$ (downwardflow), cold fluid enters which results in the decrease in global temperature. R_L and R_E are minimum at $Q_v = 0$, and increases in the right and left of $Q_v = 0$. Increasing throughflow in both directions results in stabilizing the flow. Vertical throughflow gives a temperature distribution in which gradients are significant only in the sublayer of thickness ϵ. Effective
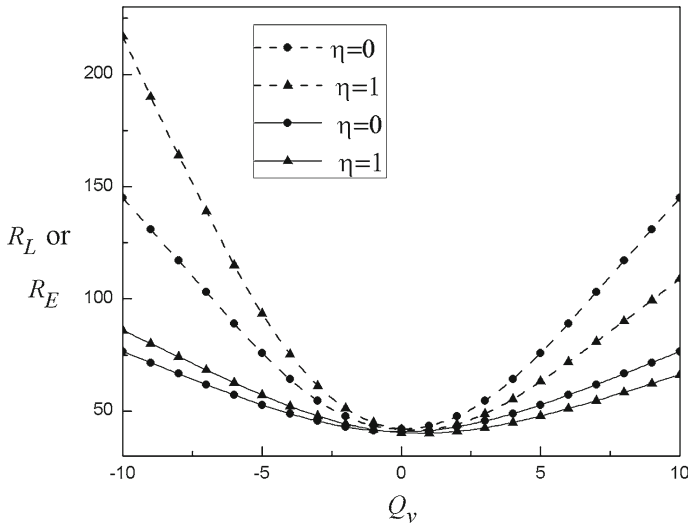
Fig. 2 Plot of R_L and R_E versus Q_v for $Pe = 0$, $R_x = 0$. *Dashed lines* are for linear theory and *solid lines* are for nonlinear theory

Rayleigh number is based on thickness of sublayer instead of the height of the porous layer H. So the bulk convection is confined to this sublayer only. Critical Rayleigh number depends on the order H/ϵ. As vertical throughflow increases, critical Rayleigh number increases. Hence, stabilization takes place. The plot for $\eta = 0$ is symmetric about $Q_v = 0$, and this symmetry breaks down when variable gravity is considered. For $Q_v < 0$ (downwardflow), flow with $\eta = 1$ is more stable than with $\eta = 0$, and for $Q_v > 0$ (upwardflow) flow with $\eta = 0$ is more stable than with $\eta = 1$. It is observed that linear and energy theories give very good agreement on critical Rayleigh numbers in absence of Q_v. But as Q_v changes in both directions, the difference between the two thresholds is widened. The linear threshold is always higher than the energy threshold. This gap is referred to as subcritical region.

Figure 3 depicts the behavior of R_L and R_E versus horizontal Peclet number Pe for $R_x = 0$, $Q_v = 0$ and $\eta = 0, 1$. In the absence of variable gravity ($\eta = 0$), direction of horizontal mass flow (the sign of Pe) has no effect on the critical Rayleigh numbers R_L and R_E, which means that graphs of R_L and R_E are symmetric about $Pe = 0$. But this symmetry breaks down as soon as η is introduced. Critical values R_L and R_E are increasing as Pe increasing from -20 to 0, but these critical values are decreasing as Pe increases from 0–20. For fixed η, it is noted that R_L in linear theory is higher than the R_E in energy theory. For $Pe < 0$, flow with $\eta = 0$ is more unstable than that with $\eta = 1$. For $Pe > 0$, flow with $\eta = 1$ is more unstable than that with $\eta = 0$.

Figure 4a, b shows the plots of R_L and R_E versus horizontal thermal Rayleigh number R_x for $Pe = 0$ and $Q_v = 1, -1$. The effect of variable gravity parameter is shown by the comparison between $\eta = 0, 1$. Increasing horizontal thermal Rayleigh number stabilizes the convection pattern in the medium. The behavior of critical Rayleigh numbers is same for $Q_v = 1$ and $Q_v = -1$. In Fig. 4a, flow with $\eta = 0$ is more stable than that with $\eta = 1$, whereas in Fig. 4b, reverse situation is observed.

Figure 5a, b represents variation of R_L and R_E against horizontal thermal Rayleigh number R_x for $Q_v = 0$, $\eta = 0, 1$, $Pe = 5$, and $Pe = -5$. When $R_x > 0$ and $Pe > 0$, basic temperature of fluid decreases in the average basic flow direction and when $R_x > 0$ and
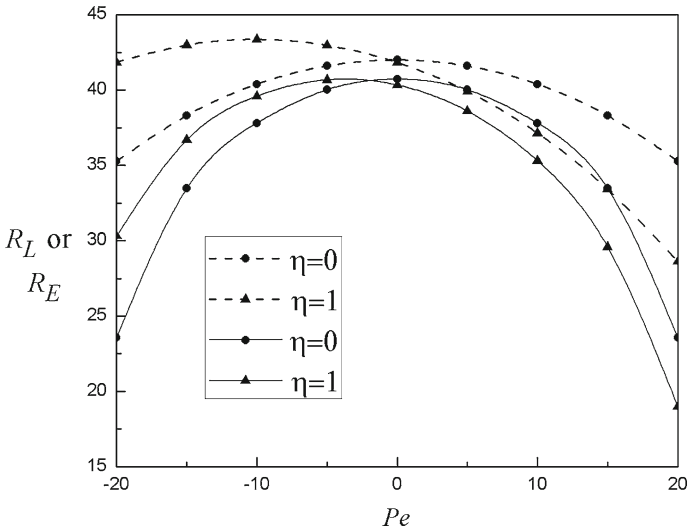
Fig. 3 Graph of R_L and R_E versus Pe for $R_x = 0$, $Q_v = 0$. *Dashed lines* are for linear theory and *solid lines* are for nonlinear theory
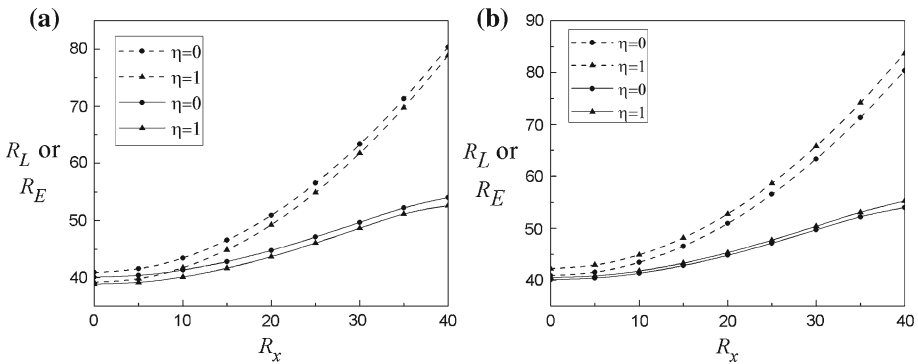

Fig. 4 Variation of R_L and R_E versus R_x for $Pe = 0$. *Dashed lines* are for linear theory and *solid lines* are for nonlinear theory. (a) $Q_v = 1$ (b) $Q_v = -1$

$Pe < 0$, reverse situation takes place. The behavior of critical vertical thermal Rayleigh numbers is same in both cases $Pe = 5$ and $Pe = -5$. In Fig. 5a, flow with $\eta = 0$ more stable than with $\eta = 1$, where as in Fig. 5b, the flow with $\eta = 1$ more stable than that with $\eta = 0$. The critical value R_L tends to increase with increasing R_x, while R_E increases up to certain values of R_x and then decreases.

From Figs. 4a, b, 5a, b, it is observed that for small values of R_x, both the linear and nonlinear thresholds have small variation in R_L and R_E. But this difference between the linear and nonlinear thresholds is increased with increasing values of R_x. It shows that for small R_x linear theory results predicts the onset of convection very well but for higher values of R_x, subcritical instabilities arise before having linear threshold.

Figure 6a, b shows the plots of R_L and R_E against R_x for $Pe = 5$, $Q_v = 1$ and $Q_v = -1$. In the presence of both vertical and horizontal Peclet numbers Q_v and Pe, the behavior of critical Rayleigh numbers is different with respect to R_x. In Fig. 6a when $Q_v = 1$, the flow
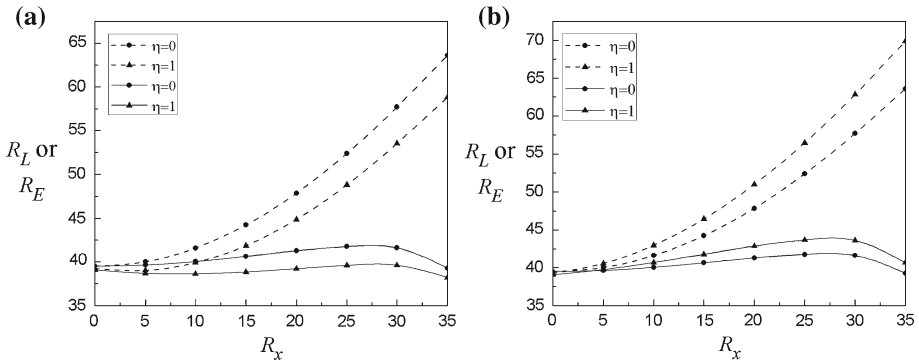
Fig. 5 Plot of R_L and R_E versus R_x for $Q_v = 0$. *Dashed lines* are for linear theory and *solid lines* are for nonlinear theory. **a** $Pe = 5$. **b** $Pe = -5$
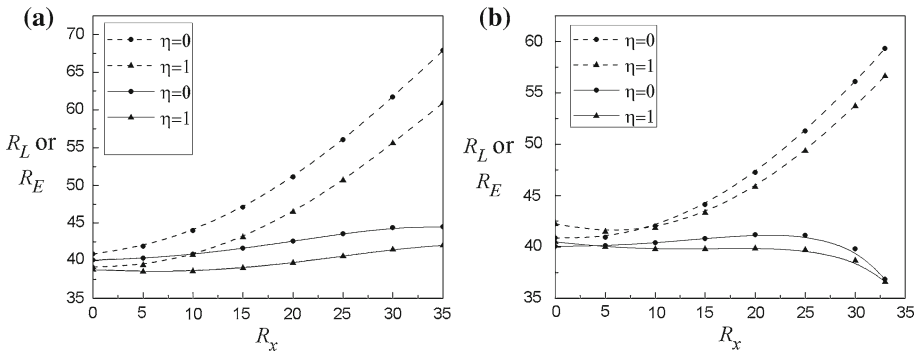

Fig. 6 Graph of R_L and R_E versus R_x. *Dashed lines* are for linear theory and *solid lines* are for nonlinear theory. **a** $Pe=5$, $Q_v=1$. **b** $Pe=5$, $Q_v=-1$

with $\eta = 0$ is more stable than that with $\eta = 1$. In Fig. 6b when $Q_v = -1$, a different response for R_L is observed with η. R_L in the presence of η is higher than the R_L in the absence of η, for small values of R_x, and this trend is reversed after certain values of R_x. Similar kind of observation is made for energy threshold. In the energy case, after certain values of R_x, the R_E decreases with R_x.

Figure 7 shows the response of R_L and R_E versus the variable gravity parameter η for $Q_v = 0, 1$, $Pe = -10, 10$. R_L and R_E are decreases as η increases. The value of critical vertical thermal Rayleigh numbers R_L and R_E is same when $Pe = 10$, $Pe = -10$ for a particular value of Q_v. In both the linear and nonlinear cases, for small values of η, the flow with $Q_v = 0$ is more unstable than the flow with $Q_v = 1$, but for sufficiently large values of η, the situation is reversed.

For both linear and energy stability results, it is commonly observed that linear stability results overshoot the nonlinear stability results. This is due to the reason that the nonlinear perturbations are neglected in the linear theory, and hence linear theory alone cannot define the complete picture of the stability. The linear stability theory gives instability boundary, whereas the nonlinear stability theory gives stability boundary. The subcritical instabilities arise in between both the boundaries. There is a great chance of having subcritical instabilities in the parameter space where linear stability results and energy stability results differ.
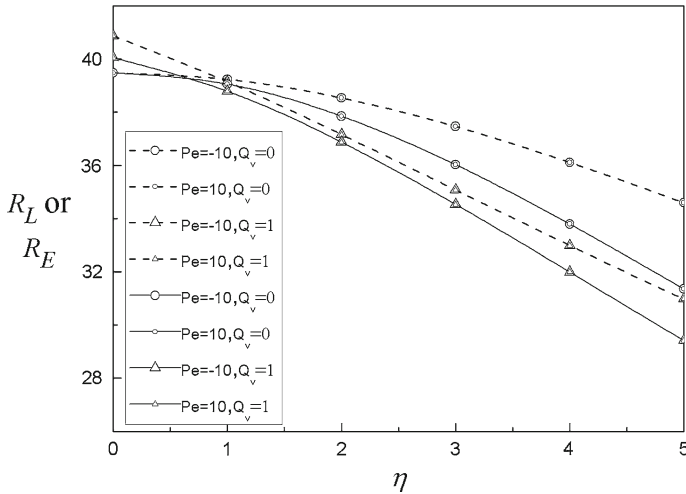
Fig. 7 Variation of R_L and R_E versus η for $R_x = 0$, $Pe = -10, 10$, $Q_v = 0, 1$. *Dashed lines* are for linear theory and *solid lines* are for nonlinear theory

6 Conclusion

The linear and nonlinear stability analyses of Hadley–Prats flow in a porous layer induced by horizontal temperature gradients are carried out by taking variable gravity and vertical throughflow into account. The eigenvalue problems are numerically integrated using shooting and Runge–Kutta methods by treating R_z as an eigenvalue. Critical thermal Rayleigh number is defined as the minimum of all R_z as wave number α varies.

In the absence of variable gravity effect, both the vertical Peclet number Q_v and horizontal Peclet number Pe have symmetric nature. For some values of Peclet numbers and variable gravity parameter η, the gap between the linear and nonlinear stability boundaries increases as R_x increases. The pattern of stability curves with respect to R_x is same irrespective of sign of Peclet number when the other Peclet number is absent. If both the Peclet numbers are present, the pattern of the stability curve differs.

References

Alex, S.M., Patil, P.R.: Effect of a variable gravity field on convection in an anisotropic porous medium with internal heat source and inclined temperature gradient. ASME J. Heat Transf. **124**, 144–150 (2002)

Alex, S.M., Patil, P.R., Venkatakrishnan, K.S.: Variable gravity effects on thermal instability in a porous medium with internal heat source and inclined temperature gradient. Fluid Dyn. Res. **29**, 1–6 (2001)

Barletta, A., Rossi di Schio, E., Storesletten, L.: Convective roll instabilities of vertical throughflow with viscous dissipation in a horizontal porous layer. Transp. Porous Media **81**, 461–477 (2010)

Brevdo, L., Ruderman, M.S.: On the convection in a porous medium with inclined temperature gradient and vertical throughflow. Part I. Normal modes. Transp. Porous Media **80**, 137–151 (2009)

Chen, F.: Throughflow effects on convective instability in superposed fluid and porous layers. J. Fluid Mech. **231**, 113–133 (1990)

Harfash, A.J.: Three-dimensional simulations for convection in a porous medium with internal heat source and variable gravity effects. Transp. Porous Media **101**, 281–297 (2014)

Homsy, G.M., Sherwood, A.E.: Convective instabilities in porous media with through flow. AlChE J. **22**, 168–174 (1976)

Horton, C.W., Rogers, F.T.: Convection currents in a porous medium. J. Appl. Phys. **16**, 367–370 (1945)

Kaloni, P.N., Qiao, Z.: Non-linear convection in a porous medium with inclined temperature gradient and variable gravity effects. Int. J. Heat Mass Transf. **44**, 1585–1591 (2001)

Kaloni, P.N., Qiao, Z.: Nonlinear convection induced by inclined thermal and solutal gradients with mass flow. Contin. Mech. Thermodyn. **12**, 185–194 (2000)

Kaloni, P.N., Qiao, Z.: Non-linear stability of convection in a porous medium with inclined temperature gradient. Int. J. Heat Mass Transf. **40**, 1611–1615 (1997)

Khalili, A., Shivakumara, I.S.: Non-darcian effects on the onset of convection in a porous layer with through-flow. Transp. Porous Media **53**, 245–263 (2003)

Lapwood, E.R.: Convection of a fluid in a porous medium. Proc. Cambridge Phil. Soc. **44**, 508–521 (1948)

Nield, D.A.: Convection in a porous medium with inclined temperature gradient. Int. J. Heat Mass Transf. **34**, 92–97 (1991)

Nield, D.A.: Convection in a porous medium with inclined temperature gradient and vertical throughflow. Int. J. Heat Mass Transf. **41**, 241–243 (1998)

Nield, D.A.: Convection induced by an inclined temperature gradient in a shallow horizontal layer. Int. J. Heat Fluid Flow **15**, 157–162 (1994)

Nield, D.A., Bejan, A.: Convection in Porous Media. Springer, New York (2013)

Nield, D.A., Kuznetsov, A.V.: The Onset of convection in a layered porous medium with vertical throughflow. Transp. Porous Media **98**, 363–376 (2013)

Prats, M.: The effect of horizontal fluid flow on thermally induced convection currents in porous medium. J. Geophys. Res. **71**, 4835–4838 (1966)

Qiao, Z., Kaloni, P.N.: Non-linear convection in a porous medium with inclined temperature gradient and vertical throughflow. Int. J. Heat Mass Transf. **41**, 2549–2552 (1998)

Rees, D.A.S., Bassom, A.P.: The onset of Darcy-Benard convection in an inclined layer heated from below. Acta Mech. **144**, 103–118 (2000)

Straughan, B.: Convection in variable gravity field. J. Math. Anal. Appl. **140**, 467–475 (1989)

Straughan, B.: The energy method, stability and nonlinear convection. Springer, New York (2004)

Sutton, F.M.: Onset of convection in a porous channel with net through flow. Phys. Fluids **13**, 1931–1934 (1970)

Weber, J.E.: Convection in a porous medium with horizontal and vertical temperature gradients. Int. J. Heat Mass Transf. **17**, 241–248 (1974)

Wooding, R.A.: Rayleigh instability of a thermal boundary layer in flow through a porous medium. Fluid Dyn. Res. **29**, 183–192 (1960)